

**Design and Synthesis of a  $C_2$ -Symmetric Self-Complementary Hydrogen-Bonding Cleft Molecule Based on the Bicyclo[3.3.1]nonane and 4-Oxo-5-azaindole Framework. Formation of Channels and Inclusion Complexes in the Solid State**

Sigitas Stončius,<sup>†</sup> Eugenius Butkus,<sup>\*,†</sup> Albinas Žilinskas,<sup>†</sup> Krister Larsson,<sup>‡</sup> Lars Öhrström,<sup>‡</sup> Ulf Berg,<sup>§</sup> and Kenneth Wärnmark<sup>\*,§</sup>

Department of Organic Chemistry, Vilnius University, Naugarduko 24, LT03225 Vilnius, Lithuania, Department of Materials and Surface Chemistry, Chalmers University of Technology, SE-412 96 Gothenburg, Sweden, and Organic Chemistry 1, Department of Chemistry, Lund University, P.O. Box 124, SE-22100 Lund, Sweden

eugenijus.butkus@chf.vu.lt; kenneth.warnmark@orgk1.lu.se

Received December 24, 2003

The synthesis of a  $C_2$ -symmetric cleft molecule **2** based on the fused framework between bicyclo[3.3.1]nonane and 4-oxo-5-azaindole, incorporating a self-complementary hydrogen-bonding motif, in both racemic and enantiomerically pure forms is reported. This cleft molecule is reminiscent of analogues of Tröger's base though with different cleft dimensions and tilt angles. The framework of **2** provides a building block for the construction of self-assembled hydrogen-bonded supramolecular structures. The solid-state structure of **2** is highly influenced by the limited solubility of ( $\pm$ )-**2** and ( $-$ )-**2**. The solvents interact with the potential hydrogen-bonding motifs of ( $\pm$ )-**2** and ( $-$ )-**2**, forming different three-dimensional structures as revealed by X-ray diffraction analysis. In the solid state ( $\pm$ )-(**2**)<sub>2</sub>·5DMF forms hydrogen-bonded pleated band structures that build up three-dimensional pens between adjacent bands in which two molecules of DMF are trapped. In contrast, the aggregate obtained from ( $-$ )-**2**, ( $-$ )-**2**·2AcOH, showed infinite bands of complex constitution.

**Introduction**

Cleft structures have attracted significant interest in supramolecular chemistry due to their ability to host guests and to allow for functional groups to be oriented in well-defined spatial arrangement.<sup>1</sup> In particular, analogues of Tröger's base<sup>2</sup> (Figure 1) have emerged as a valuable building block for the construction of a number of chiral host systems for molecular recognition studies. The use of functionalized anilines in the synthesis of the chiral cavity of the Tröger's base has led to development of a range of receptors for recognition of various compounds.<sup>3</sup> Thus, molecular tweezers with bis- and tris-Tröger's base skeleton<sup>4</sup> as well as carbocyclic analogues of the Tröger's base, such as Kagan's ether<sup>5</sup> and the dibenzobicyclo[*b,f*][3.3.1]nona-5a,6a-diene framework,<sup>6</sup> have been reported.

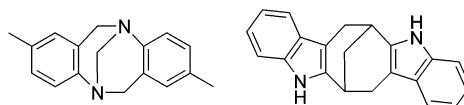


**FIGURE 1.** Tröger's base<sup>8</sup> (left) and methanocycloocta[1,2-*b*:5,6-*b'*]diindole (right).

Recently we reported on the Fischer indole synthesis of methanocycloocta[1,2-*b*:5,6-*b'*]diindole (Figure 1) from bicyclo[3.3.1]nonane-2,6-dione **1**.<sup>7</sup> This chiral,  $C_2$ -symmetric molecule is reminiscent of Tröger's base by its cleft-like geometry and the arrangement of the aromatic rings in space (Figure 1), which creates a rigid chiral cavity.

The molecular shape of bicyclo[3.3.1]nonane itself<sup>9</sup> has been shown to be suitable to form self-assembled supramolecular structures and inclusion complexes with guests containing a diverse range of functionality. Following this line, bicyclo[3.3.0]octane diquinoline<sup>10</sup> and

\* To whom correspondence should be addressed. Fax: (for E.B.) 370-5-2330987 and (for K.W.) +46-46-2224119.

<sup>†</sup> Vilnius University.

<sup>‡</sup> Chalmers University of Technology.

<sup>§</sup> Lund University.

(1) Rebek, J., Jr. *Angew. Chem. Int. Ed., Engl.* **1990**, *29*, 245–255. (2) Demeunynck, M.; Tatibouët, A. Recent development in Tröger's base chemistry. In *Progress in Heterocyclic Chemistry*; Gribble, G. W., Gilchrist, T. L., Eds.; Pergamon: Oxford, 1999; Vol. 11, pp 1–21.

(3) (a) Goswami, S.; Ghosh, K.; Dasgupta, S. *J. Org. Chem.* **2000**, *65*, 1907–1914. (b) Hansson, A. P.; Norrby, P.-O.; Wärnmark, K. *Tetrahedron Lett.* **1998**, *39*, 4565–4568. (c) Goswami, S.; Ghosh, K. *Tetrahedron Lett.* **1997**, *38*, 4503–4506. (d) Crossley, M. J.; Hambley, T. W.; Mackay, L. G.; Try, A. C.; Walton, R. J. *J. Chem. Soc., Chem. Commun.* **1995**, 1077–1079. (e) Crossley, M. J.; Mackay, L. G.; Try, A. C. *J. Chem. Soc., Chem. Commun.* **1995**, 1925–1927. (f) Adrian, J. C., Jr.; Wilcox, C. S. *J. Am. Chem. Soc.* **1992**, *114*, 1398–1403. (g) Adrian, J. C., Jr.; Wilcox, C. S. *J. Am. Chem. Soc.* **1989**, *111*, 8055–8057.

(4) (a) Valík, M.; Dolensky, B.; Petříčková, H.; Král, V. *Collect. Czech. Chem. Commun.* **2002**, *67*, 609–621. (b) Pardo, C.; Sesiñlo, E.; Gutiérrez-Puebla, E.; Monge, A.; Elguero, J.; Fruchier, A. *J. Org. Chem.* **2001**, *66*, 1607–1611.

(5) Kagan, J.; Chen, S.-Y.; Agdeppa, D. A., Jr.; Watson, W. H.; Zabel, V. *Tetrahedron Lett.* **1977**, *51*, 4469–4470.

(6) (a) Field, J. D.; Turner, P.; Harding, M. M.; Hatzikominos, T.; Kim, L. *New J. Chem.* **2002**, *26*, 720–725. (b) Kimber, M. C.; Try, A. C.; Painter, L.; Harding, M. M.; Turner, P. *J. Org. Chem.* **2000**, *65*, 3042–3046. (c) Try, A. C.; Painter, L.; Harding, M. M. *Tetrahedron Lett.* **1998**, *39*, 9809–9812. (d) Shi, X.; Miller, B. *J. Org. Chem.* **1995**, *60*, 5714–5716.

(7) Butkus, E.; Berg, U.; Malinauskienė, J.; Sandström, J. *J. Org. Chem.* **2000**, *65*, 1353–1358.

bicyclo[3.3.1]nonane diquinoxaline<sup>11</sup> lattice inclusion hosts have been developed by Bishop.

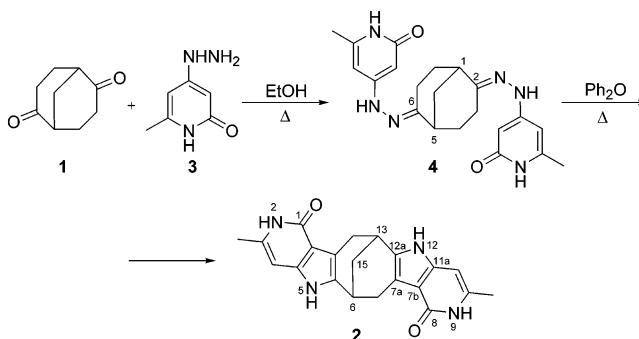
Analogous carbocyclic methanocyclooctadiindole structures could provide access to novel chiral  $C_2$ -symmetric clefts reminiscent to Tröger's base though with different cleft dimensions and tilt angles. In particular, in contrast to Tröger's base, frameworks based on bicyclo[3.3.1]nonane are relatively easy obtained in optically pure form<sup>7,12</sup> and are stable to racemization in weak acid. Moreover, clefts of this framework incorporating appropriately positioned hydrogen-bonding sites may serve as building blocks for the construction of self-assembled helical supramolecular structures. Because the helical self-assembly is a structural feature predominant and so important in Nature, artificial helical architectures have been actively sought.<sup>13</sup>

Considering the foregoing, we report on the design and synthesis of a novel cleft structure based on bicyclo[3.3.1]nonane fused with 4-oxo-5-azaindole, specifically, chiral molecular cleft **2** incorporating self-complementary hydrogen-bonding sites in both racemic and enantiomerically pure forms. Geometric features as well as aggregation of ( $\pm$ )-**2** and ( $-$ )-**2** in the solid state were characterized by X-ray diffraction analysis.

## Results and Discussion

**Synthesis.** For design of the molecular clefts incorporating hydrogen-bonding sites, suitable moieties having respective functional groups for hydrogen-bonding should be introduced. This may be realized by using an appropriate heterocyclic hydrazine in the Fischer indolization reaction. The 2(*1H*)-pyridinone (2-pyridone) structure seemed to be suitable for that purpose as a result of its well-documented ability to form noncovalently bonded associates via self-complementary donor–acceptor (D–A) hydrogen-bonding array.<sup>14</sup> The above-mentioned fragment also attracted our attention because it is found in the bicyclo[3.3.1]nonane-based alkaloid huperzine A, a reversible inhibitor of acetylcholinesterase (AChE), which is a potent drug for treatment of the Alzheimer's disease.<sup>15</sup>

## SCHEME 1



The synthesis of the cleft molecule containing the self-complementary 2-pyridone motif, **2**, is outlined in Scheme 1 and involves the Fischer indole synthesis as the key step. Hydrazine **3** was obtained in two steps from commercially available 4-hydroxy-6-methyl-2(*1H*)-pyran-2-one according to the procedures described in the literature.<sup>16,17</sup>

The reaction of racemic 2,6-dione **1** with hydrazine **3** in refluxing ethanol afforded the corresponding racemic bishydrazone **4** (Scheme 1) as a mixture of configurational *E,E* and *E,Z* isomers as evidenced by <sup>1</sup>H and <sup>13</sup>C NMR spectroscopy: In the <sup>13</sup>C NMR spectrum two sets of signals were observed in the aliphatic region; resonance signals of C=N and some heteroaromatic carbon atoms were doubled as well. Four resonances corresponding to the bicyclic skeleton CH<sub>2</sub> and CH carbon atoms in the <sup>13</sup>C NMR spectrum confirm the structure of the major *E,E* isomer with  $C_2$  symmetry, whereas the minor non-symmetric *E,Z* isomer exhibits seven resonances in the aliphatic region of the carbons of the bicyclic skeleton. The *E,E* and *E,Z* isomers are practically indistinguishable in the <sup>1</sup>H NMR spectrum by contrast. The exceptions were the resonance signals of the protons of the =N–NH– fragment, which appeared as two separate singlets at  $\delta = 9.35$  and 9.19 ppm for the *E* and *Z* isomers, respectively, in the ratio 1.73:0.27.

Subsequent thermal Fischer indole cyclization of racemic bishydrazone **4** in boiling diphenyl ether under nitrogen atmosphere afforded target structure **2**. It should be noted that ( $\pm$ )-**2** is insoluble in most common organic solvents and only slightly soluble in DMF and DMSO. Crude ( $\pm$ )-**2** could be recrystallized only from glacial acetic acid, giving aggregates of ( $\pm$ )-**2** with acetic acid in a ratio 1:1 (as demonstrated from integration in the <sup>1</sup>H NMR spectrum). This is not surprising, as 2-pyridone itself readily forms cocrystals with various dicarboxylic acids.<sup>18</sup> Attempts to remove the complexed acetic acid have failed.

The structure of ( $\pm$ )-2,9-diaza-3,10-dimethyl-1,8-dioxo-2,5,6,7,9,12,13,14-octahydro-6,13-methanocycloocta[1,2-*b*:5,6-*b'*]diindole<sup>19</sup> **2** was assigned on the basis of spectroscopic data and confirmed by X-ray diffraction analysis. Seven groups of proton resonances and 11 distinct carbon

(8) Tröger, J. *J. Prakt. Chem.* **1887**, *36*, 225–245.  
 (9) (a) Bishop, R. *Synlett* **1999**, 1351–1358. (b) Ung, A. T.; Bishop, R.; Craig, D. C.; Dance, I. G.; Scudder, M. L. *J. Chem. Soc., Perkin Trans. 2* **1992**, 861–862.  
 (10) (a) Rahman, A. N. M. M.; Bishop, R.; Craig, D. C.; Scudder, M. L. *Eur. J. Org. Chem.* **2003**, 72–81. (b) Rahman, A. N. M. M.; Bishop, R.; Craig, D. C.; Scudder, M. L. *Chem. Commun.* **1999**, 2389–2390.  
 (11) Marjo, C. E.; Bishop, R.; Craig, D. C.; Scudder, M. L. *Eur. J. Org. Chem.* **2001**, 863–873.  
 (12) (a) Butkus, E.; Malinauskienė, J.; Stončius, S. *Org. Biomol. Chem.* **2003**, *1*, 391–394. (b) Butkus, E.; Malinauskienė, J.; Orentas, E.; Žilinskas, A. *Synth. Commun.* **2003**, *33*, 1595–1602. (c) Butkus, E.; Žilinskas, A.; Stončius, S.; Rozenbergas, R.; Urbanová, M.; Setnická, V.; Bouř, P.; Volka, K. *Tetrahedron: Asymmetry* **2002**, *13*, 633–638. (d) Butkus, E.; Stončius, S.; Žilinskas, A. *Chirality* **2001**, *13*, 694–698.  
 (13) (a) Blay, G.; Fernández, I.; Pedro, J. R.; Ruiz-García, R.; Muñoz, M. C.; Cano, J.; Carrasco, R. *Eur. J. Org. Chem.* **2003**, 1627–1630. (b) Dapporto, P.; Paoli, P.; Roelens, S. *J. Org. Chem.* **2001**, *66*, 4930–4933. (c) Berl, V.; Huc, I.; Khoury, R. G.; Krische, M. J.; Lehn, J.-M. *Nature* **2000**, *407*, 720–723. (d) Berl, V.; Huc, I.; Khoury, R. G.; Lehn, J.-M. *Chem. Eur. J.* **2001**, *7*, 2798–2809. (e) Berl, V.; Huc, I.; Khoury, R. G.; Lehn, J.-M. *Chem. Eur. J.* **2001**, *7*, 2810–2820. (f) Yue, W.; Bishop, R.; Scudder, M. L.; Craig, D. C. *J. Chem. Soc., Perkin Trans. 1* **1997**, 2937–2946. (g) Piguet, C.; Bernardinelli, G.; Hopfgartner, G. *Chem. Rev.* **1997**, *97*, 2005–2062.  
 (14) (a) Ducharme, Y.; Wuest, D. J. *J. Org. Chem.* **1988**, *53*, 5787–5789. (b) Simard, M.; Su, D.; Wuest, D. *J. Am. Chem. Soc.* **1991**, *113*, 4696–4698. (c) Boucher, E.; Simard, M.; Wuest, D. *J. Org. Chem.* **1995**, *60*, 1408–1412.

(15) Kozikowski, A. P.; Tuckmantel, W. *Acc. Chem. Res.* **1999**, *32*, 641–650.  
 (16) Wang, C.-S. *J. Heterocycl. Chem.* **1970**, *7*, 389–392.  
 (17) Bisagni, E.; Ducrocq, C.; Civier, A. *Tetrahedron* **1976**, *32*, 1383–1390.  
 (18) (a) Edwards, M. R.; Jones, W.; Motherwell, W. D. S. *Cryst. Eng.* **2002**, 25–36. (b) Aakeröy, C. B.; Beatty, A. M.; Nieuwenhuysen, M.; Zou, M. *Tetrahedron* **2000**, *56*, 6693–6699.

**TABLE 1. Hydrogen Bond Geometry for ( $\pm$ )-(2)<sub>2</sub>-5DMF, Aggregate 5, Compared to the Dimer of 2-Pyridone**

donor	hydrogen	acceptor	D...A (Å)	$\angle$ DHA (deg) <sup>c</sup>
N(1)	H(1N)	O(1)	2.806(3)	151.38(16)
N(4)	H(4N)	O(2)	2.868(3)	170.12(17)
N(2)	H(2N)	O(100) <sup>a</sup>	2.847(4)	167.78(16)
N <sup>b</sup>	H <sup>b</sup>	O <sup>b</sup>	2.773(4) <sup>b</sup>	158.87(49)

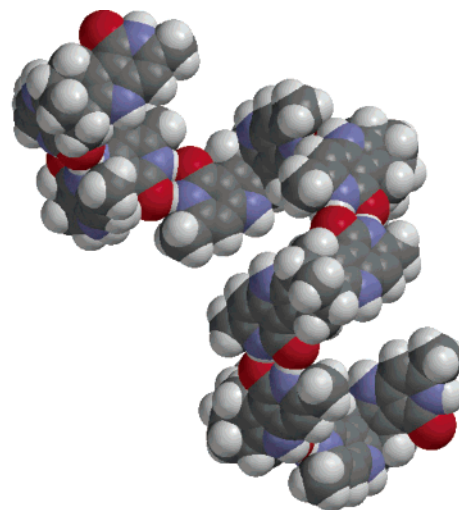
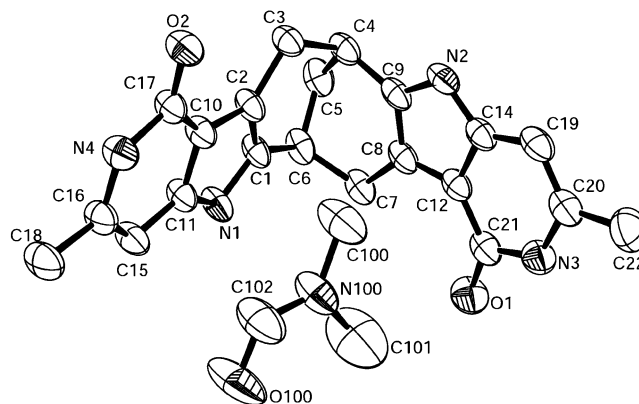
<sup>a</sup> DMF oxygen; <sup>b</sup> X-ray diffraction data for 2-pyridone dimer;<sup>24</sup>  
<sup>c</sup> D–H in the 2-pyridone plane.

atoms resonances in the <sup>1</sup>H and <sup>13</sup>C NMR spectra, respectively, confirm the formation of the C<sub>2</sub>-symmetric structure. The cyclization pathway to pyrrolo[3,2-*c*]pyridin-4-one heterosystem in **2** is in accordance with earlier literature data on the cyclization of 4-hydrazino-2(1*H*)-pyridinone hydrazones.<sup>17,20</sup>

An efficient resolution of enantiomers of bicyclo[3.3.1]-nonane-2,6-dione **1** by baker's yeast<sup>21</sup> giving the (+)-(1*S*,5*S*)-enantiomer offers a crucial chiral structure on the route to novel enantiomerically pure C<sub>2</sub>-symmetric molecular clefts such as **2**. Thus, starting from diketone (+)-**1** (>99% ee),<sup>22</sup> enantiomerically pure (–)-**2** was obtained in two steps by applying the same synthetic methodology as for ( $\pm$ )-**2** (Scheme 1). The absolute configuration of (–)-**2** is predetermined by the configuration of the starting (+)-(1*S*,5*S*)-dione **1** since the configuration of the bridgehead atoms does not change during the hydrazone formation and the subsequent indolization reactions. However, the priority in the sequence of the substituents changes in the diindole structure **2**, and therefore we define the configuration of (–)-diindole as (6*R*,13*R*)-**2**. Enantiomerically pure (–)-**2** turned out to be somewhat more soluble compared to ( $\pm$ )-**2** but still totally insoluble in nonpolar aprotic solvents.

**Molecular Modeling.** Self-assembly of enantiomerically pure **2** via self-complementary 2-pyridone motifs might form a homochiral helical supramolecular structure as suggested by molecular modeling using the semiempirical PM3 method.<sup>23</sup> Calculated hydrogen bond length (O...N) and angle O...H–N are 2.815 Å and 177°, respectively, compared to 2.77 Å (N...O) and 159° (Table 1) as determined by X-ray diffraction analysis of the 2-pyridone dimer.<sup>24</sup> The energy optimized geometry of such homochiral heptameric assembly consisting of (6*S*,13*S*)-**2** is presented in Figure 2.

More specifically, association of (6*S*,13*S*)-**2** would lead to the formation of a right-handed (P) helix, whereas (6*R*,13*R*)-**2** upon association should give a left-handed (M) helix with approximately four associated molecules in one turn. In contrast, ( $\pm$ )-**2** is expected to aggregate either

**FIGURE 2.** PM3-optimized geometry of a proposed homochiral helical assembly of (6*S*,13*S*)-**2**.**FIGURE 3.** ORTEP plot and numbering scheme of ( $\pm$ )-(2)<sub>2</sub>-5DMF, here represented by one of the two heterochiral molecules, (6*S*,13*S*)-**2**, constituting aggregate **5**. Disordered DMF molecules are omitted.

to helical assemblies as above, including both left- and right-handed helices, or to pleated zigzag structures consisting of alternating (6*S*,13*S*)-**2** and (6*R*,13*R*)-**2**. Last, the spontaneous resolution of ( $\pm$ )-**2** in the solid state and formation of the enantiomorphous crystals containing homochiral helices may be envisaged. Calculations on the heterochiral dimer **2**·**2** gave negligible hydrogen bond energy difference compared to the homochiral dimer with identical length and angle of hydrogen bonds. Nevertheless, by using one single enantiomer it should be possible to control both the chirality and three-dimensional structure of the resulting supramolecular assembly.

**X-ray Crystallography. Crystal Structure of ( $\pm$ )-(2)<sub>2</sub>-5DMF; Aggregate 5.** Single crystals of ( $\pm$ )-**2** suitable for X-ray analysis were obtained by recrystallization from DMF. The resulting X-ray structure of **5** revealed two equivalent but heterochiral cleft molecules **2** and five DMF molecules (three of them disordered) in the unit cell.

**Intramolecular Structural Properties of 5.** The rigid cleft shape of **2** is revealed in Figure 3, in which the ORTEP view of one of the two heterochiral molecules in the unit cell, (6*S*,13*S*)-**2** constituting aggregate **5**, is

(19) The IUPAC name for structure **2** is 6,17-dimethyl-3,7,14,18-tetraazahexacyclo[10.10.1.0<sup>2,10</sup>.0<sup>4,9</sup>.0<sup>13,21</sup>.0<sup>15,20</sup>]tricoso-2(10),4(9),5,13-(21),15(20),16-hexaene-8,19-dione.

(20) (a) Bisagni, E.; Huang, N.-C. *Tetrahedron* **1986**, *42*, 2303–2309. (b) Bisagni, E.; Nguyen, C.-H.; Pierre, A.; Pepin, O.; de Cointet, P.; Gros, P. *J. Med. Chem.* **1988**, *31*, 398–405. (c) Harada, K.; Someya, H.; Zen, S. *Heterocycles* **1994**, *38*, 1867–1880.

(21) Hoffmann, G.; Wiartalla, R. *Tetrahedron Lett.* **1982**, *23*, 3887–3888.

(22) ee determined on BetaDex 120 capillary column as described earlier: Berg, U.; Butkus, E.; Frejd, T.; Stončius, A. *Acta Chem. Scand.* **1997**, *51*, 1030–1034.

(23) SPARTAN Pro, version 1.0.5; Wavefunction, Inc.: 1840 Von Karman Avenue, Suite 370, Irvine, CA 92612.

(24) Ohms, U.; Guth, H.; Hellner, E.; Dannohl, H.; Schweig, A. Z. *Kristallogr.* **1984**, *169*, 185.

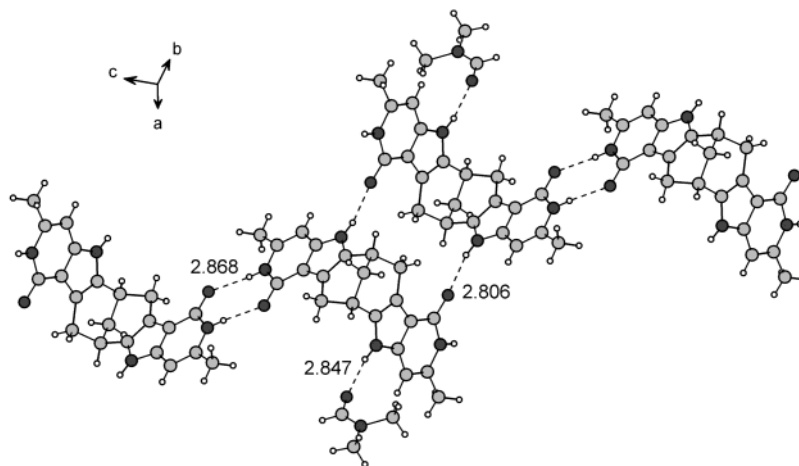


**FIGURE 4.** Hydrogen bond network in the crystal structure of  $(\pm)$ -**(2)**<sub>2</sub>·5DMF, aggregate **5**. Only hydrogen-bonded DMF molecules are displayed. The bond distances are between N···O.

displayed. The most important structural feature of this type of bicyclic framework is the angle between the two aromatic planes in **2** (given as least-squares planes), defining the chiral cleft. For the molecule (6*S*,13*S*)-**2** in aggregate **5**, this value is 87.75°. For the most similar Tröger's base analogue to **2**, namely, the bis(*N*-methyl pyrrole) analogue of Tröger's base, X-ray diffraction analysis determined this angle to 104.17°. <sup>25</sup>

**Intermolecular Band Structure Built in Aggregate 5.** The crystal structure of aggregate **5** reveals the formation of an infinite hydrogen-bonded chain along the [0 -1 1] diagonal (Table 1 and Figure 4), where two distinct hydrogen bond types are observed: Two molecules of the opposite sense of chirality are linked by hydrogen bonds using one of the two self-complementary 2-pyridone motifs in molecule **2**, resulting in heterochiral dimers. As seen in Table 1, the distances of the hydrogen bond in the 2-pyridone motif of **5** is longer than in 2-pyridone itself. Obviously other forces (inter- or intramolecular) are acting in the more complex aggregate **5** than in the dimer of 2-pyridone. The so formed heterochiral dimers are interlinked by hydrogen bonds formed between the hydrogen atom of one of the two pyrrole ring nitrogen in one molecule **2** and the carbonyl group of one of the other 2-pyridone unit in the neighboring molecule **2** of opposite chirality. Each layer of this network comprises a pleated band (compare  $\beta$ -pleated sheets of polypeptide chains).<sup>26</sup> Each molecule of **2** constituting the aggregate **5** is also hydrogen-bonded to DMF via a hydrogen bond between the hydrogen atom of the other pyrrole ring nitrogen and the carbonyl group of DMF (Figure 4).

**Three-Dimensional Network and Inclusion Complexes Built Up from the Band Structure in Aggregate 5.** The crystal structure of aggregate **5** revealed that the molecular clefts of **2** are lattice inclusion hosts: Two molecules from two adjacent pleated hydrogen-bonded bands comprise a molecular cage (pen),<sup>10</sup> where the heteroaromatic rings of **2** act as a surrounding fences. Each rhomboid pen is identical and is composed of two

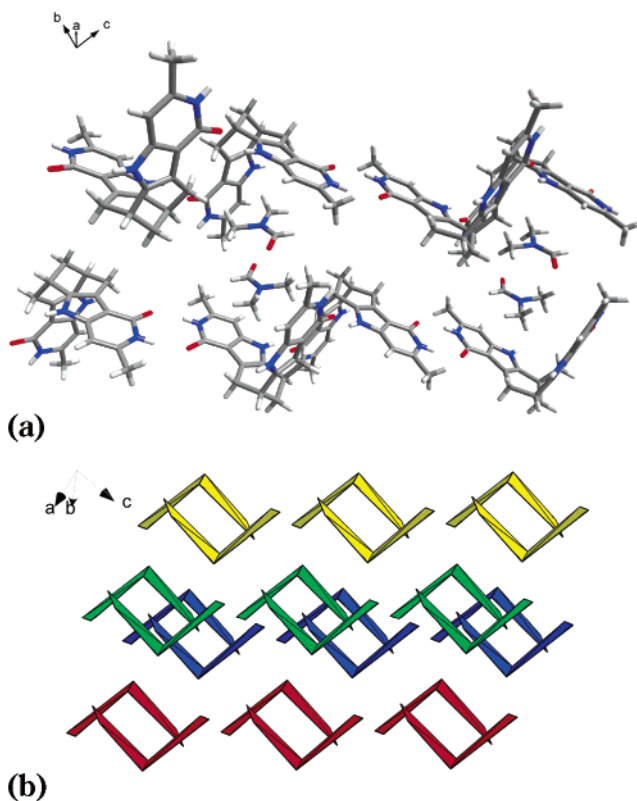


**FIGURE 5.** Crystal structure of  $(\pm)$ -**(2)**<sub>2</sub>·5DMF, aggregate **5**. (a) Molecular pens formed by the adjacent hydrogen-bonded networks with two DMF molecules located in each pen. Disordered DMF molecules are omitted. (b) Schematic representation of the molecular pens. DMF molecules are omitted.

heterochiral molecules of **2**. The so-formed void is occupied by two molecules of DMF (Figure 5a).

In this way parallel planar arrays of pens, almost perpendicular to hydrogen-bonded networks, are formed throughout the crystal lattice (Figure 6a). The packing of pens in layers is assisted by heteroaryl face-C-H (aliphatic) interactions<sup>27</sup> between *exo* faces of adjacent pens. This interaction is observed between the C(5)-H

(25) Valík, M.; Dolensky, B.; Petříčková, H.; Vašek, P.; Král, V. *Tetrahedron Lett.* **2003**, *44*, 2083–2086.

(26) Lehninger, A. L.; Nelson, D. L.; Cox, M. M. *Principles of Biochemistry*, 2nd ed.; Worth Publishers, New York, 1993.

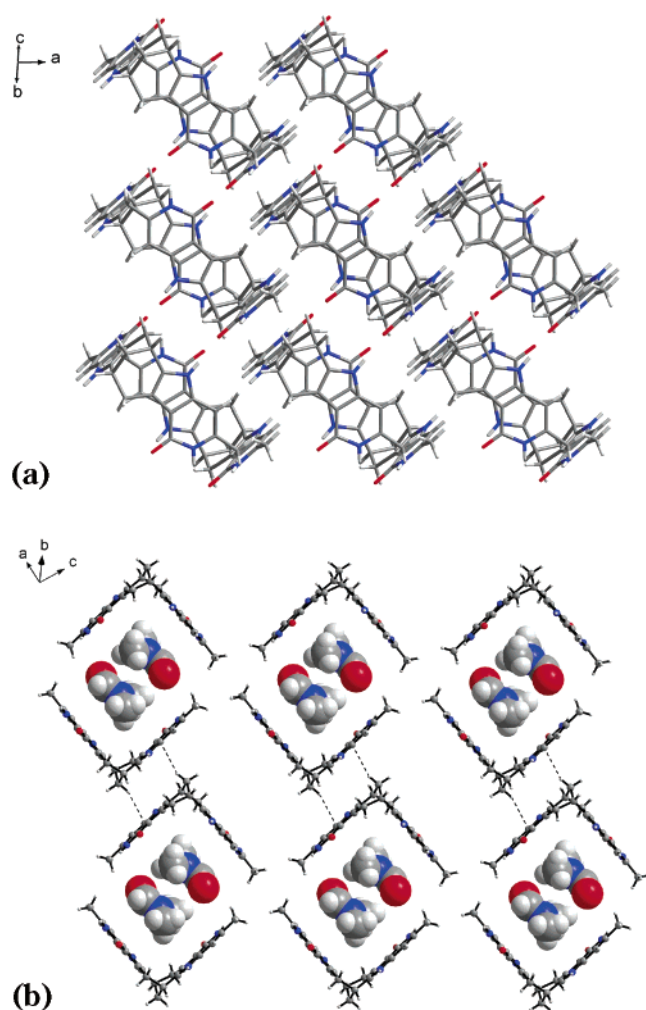


**FIGURE 6.** Crystal structure of  $(\pm)$ -**2**·5DMF, aggregate **5**. (a) Planar arrays of pens, side view. (b) Top view of part of a layer of molecular pens and their included DMF guests. Aryl face-CH interactions are indicated by dashed lines.

atom and one pyrrole ring with a C–C atom centroid distance of 3.74(5) Å, as illustrated in Figure 6b.

The cavities of the molecular pens are large enough to enclose two DMF molecules as guests, which almost entirely fill the void (Figure 6b). The DMF guest molecules are arranged in the antiparallel fashion in respect to each other but not parallel to the heteroaromatic fences of the host. Interplanar distance between planes defined by the DMF molecules is found to be 3.9 Å. The two carbonyl groups of the two stacked guest molecules point in opposite directions reaching outward of the cavity and are hydrogen-bonded (pyrrole N–H···O=C), as demonstrated by the short N–O distance of 2.85(3) Å (Table 1).

Additionally, *exo*-faces of the host from adjacent hydrogen-bonded networks comprise channels along the *a* axis filled with disordered DMF molecules (Figure 7). These channels occupy 28% of the unit cell volume (PLATO<sup>28</sup> analysis).

(27) (a) Nguyen, V. T.; Rahman, A. N. M. M.; Bishop, R.; Craig, D. C.; Scudder, M. L. *Aust. J. Chem.* **1999**, *52*, 1047–1053. (b) Marjo, C. E.; Scudder, M. L.; Craig, D. C.; Bishop, R. *J. Chem. Soc., Perkin Trans. 2* **1997**, 2099–2104.

(28) Spek, A. L. *Acta Crystallogr.* **1990**, *A46*, C34.

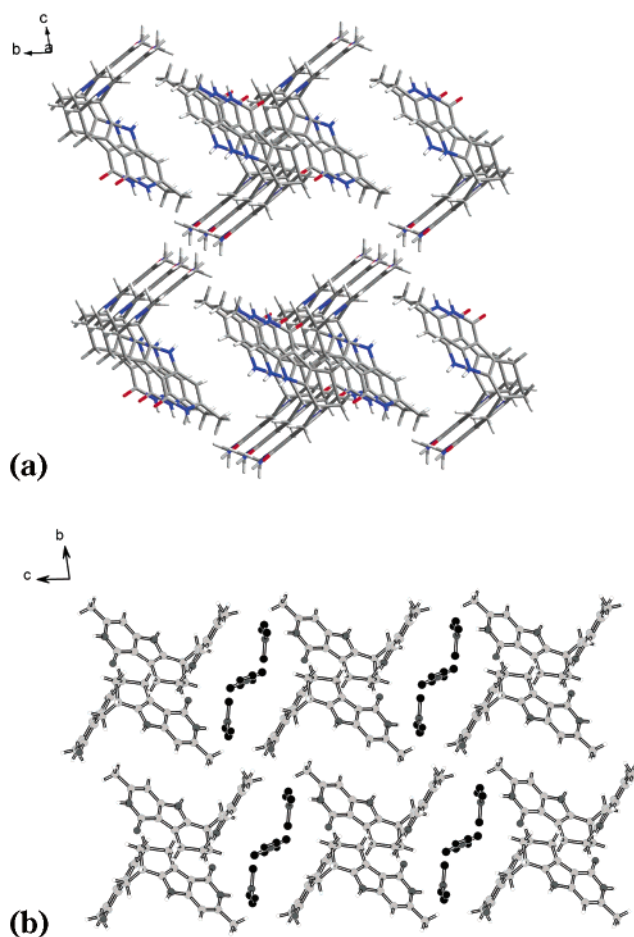


**FIGURE 7.** Crystal structure of  $(\pm)$ -**2**·5DMF, aggregate **5**. (a) Channel along the *a* axis formed by *exo*-faces of the host. Disordered DMF molecules are omitted. (b) View of the channels with disordered DMF molecules (in black) included.

#### Crystal Structure of (–)-**2**·2AcOH; Aggregate **6**.

Single crystals of (–)-**2** could only be obtained by vapor diffusion of ether to a solution of (–)-**2** in acetic acid. Unfortunately, in this case self-association of (–)-**2** via 2-pyridone motifs is fully thwarted by association of the latter fragments with acetic acid. The resulting X-ray structure of **6** revealed two different crystallographic fragments of cleft molecules (–)-**2** and four molecules of acetic acid in the unit cell. ORTEP representations of the two fragments of (–)-**2** and acetic acid in the asymmetric unit of aggregate **6** are shown in Figure 8. The angle between the two aromatic planes in **2** (given as least-squares planes), defining the cleft is 92.11° for fragment A and 90.20° for fragment B.

Like the crystal structure of aggregate **5**, obtained from  $(\pm)$ -**2**, the crystal structure of the aggregate **6**, obtained from enantiomerically pure compound (–)-**2**, also contains infinite chains, but these are more complex. The aggregate contains two different types of acetic acid: bridging, which are involved in the hydrogen-bonded chain propagation, and terminating, ending the chain. Acetic acid molecules are coordinated to 2-pyridone fragments of **2** via two hydrogen bonds between N–H···O=C and C=O···H–O. Furthermore, the aggregate consist of “embraced” dimers of (–)-**2** connected through

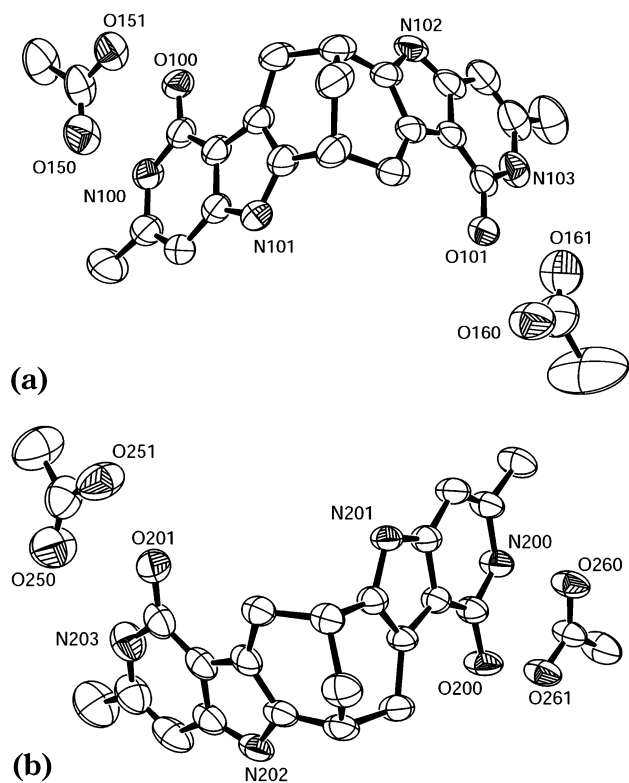


**FIGURE 8.** Crystal structure of  $(-)-2 \cdot 2\text{AcOH}$ , aggregate **6**. ORTEP view of the two fragments A (a) and B (b) containing  $(-)-2$  and acetic acid.

two hydrogen bonds between a pyrrole N–H in one molecule and the carbonyl group of a 2-pyridone fragment in an adjacent molecule with  $\text{N}\cdots\text{O}$  distances of 2.97 and 3.125 Å, respectively. The 2-pyridone motifs involved in this interaction are also hydrogen-bonded to the terminating molecules of the acetic acid. The so-formed dimer is linked through the bridging acetic acid molecules to the neighboring dimers. This is shown in Figure 9, where the acetic acid molecules involved in bridges are shown in gray. The distances of the hydrogen bonds can be found in Table 2.

Each bridging acetic acid molecule is involved in four hydrogen bonds, namely, two to the 2-pyridone motif of the one dimeric unit of  $(-)-2$  and one  $\text{N}-\text{H}\cdots\text{O}=\text{C}$  bond to each of two symmetry related adjacent dimeric units of  $(-)-2$  (see Figure 10a). The chains extend along the  $b$  axis, and a schematic side view is shown in Figure 10b, which also includes the bridging acetic acid molecules. The packing of the chains along the same axis results in channels shown in Figure 11, which occupy 16% of the unit cell volume (PLATO analysis<sup>28</sup>).

A similar feature observed for both  $(\pm)-2$  and  $(-)-2$  is the participation of the pyrrole ring N–H atoms in the self-association of **2**. Hydrogen-bonding observed between a pyrrole N–H and the carbonyl group of a 2-pyridone fragment is a significant contributor to the lattice packing and determines three-dimensional structure of the resulting aggregates **5** and **6**. Formation of the supramolecular structures via self-association of the N-5(12) alkylated analogues of **2**, where hydrogen-bonding should occur solely between self-complementary 2-pyridone fragments, is currently under investigation.

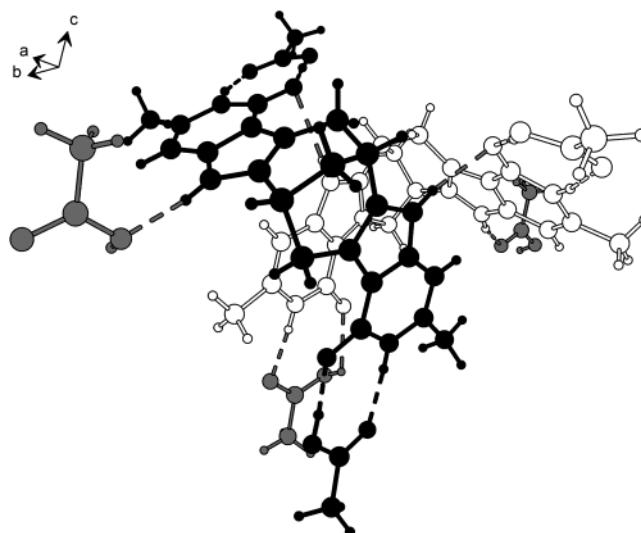


**FIGURE 9.** Crystal structure of  $(-)-2 \cdot 2\text{AcOH}$ , aggregate **6**. The two fragments in the dimer are colored white and black. Grey molecules are the molecules of acetic acid involved in the bridge.

**TABLE 2.** Hydrogen Bond Distances for  $(-)-2 \cdot 2\text{AcOH}$ , Aggregate **6**

atoms <sup>a</sup>	distance (Å)
N(100)–O(150)	2.833(6)
N(101)–O(201)	2.970(6)
N(102)–O(261)	2.803(5)
N(103)–O(161)	2.931(8)
N(200)–O(260)	2.723(6)
N(201)–O(101)	3.125(5)
N(202)–O(260)	2.883(5)
N(203)–O(250)	2.925(8)
O(151)–O(100)	2.539(6)
O(160)–O(101)	2.548(6)
O(251)–O(201)	2.536(6)
O(261)–O(200)	2.479(5)

<sup>a</sup> See Figure 8 for numbering

## Conclusions

The synthesis of a  $C_2$ -symmetric molecular cleft **2**, containing an all-carbon bicyclo[3.3.1]nonane skeleton, incorporating the self-complementary hydrogen-bonding 2-pyridone motif, in both racemic and enantiomerically pure forms, has been accomplished. This chiral cleft possesses complementary yet unique features compared to analogues of Tröger's base. Geometric features and aggregation of **2** in hydrogen-bonded networks, both as racemate  $(\pm)-2$  and as optically pure  $(-)-2$ , and formation of a lattice inclusion compound in the solid state were revealed by single-crystal X-ray diffraction analysis. Hydrogen-bonding observed between a pyrrole N–H and the carbonyl group on a 2-pyridone fragment is significant contributor to the lattice packing for both  $(\pm)-2$  and  $(-)-2$  and determines the three-dimensional structure of the resulting supramolecular aggregates. An additional factor is the choice of the solvents for crystallization, governed by the poor solubility of **2**.

## Experimental Section

**Crystallographic Data Collection and Structure Determination of Aggregate 5 (from  $(\pm)-2$ ) and Aggregate 6 (from  $(-)-2$ ).** Crystallographic measurements of aggregates

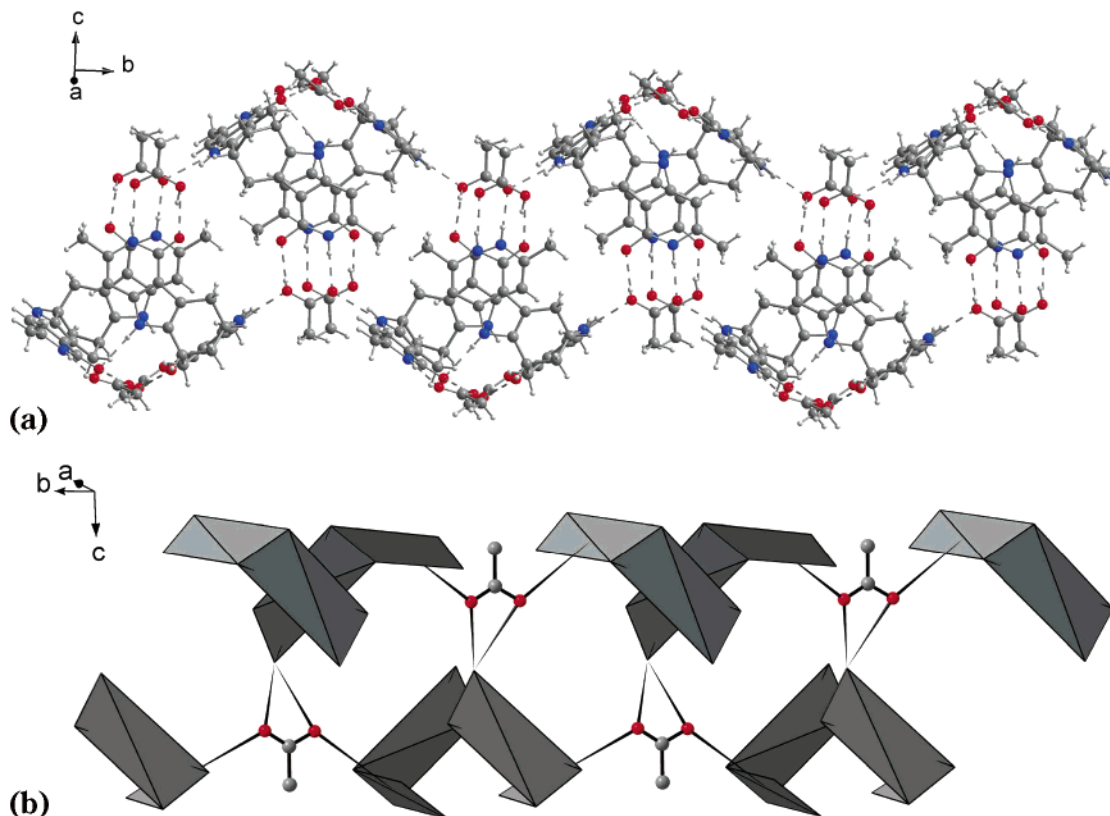


**FIGURE 10.** Crystal structure of  $(-)$ -**2**·**2AcOH**, aggregate **6**. (a) Side view of the chain. (b) Schematic representation of the chain. Terminating acetic acid molecules are omitted.

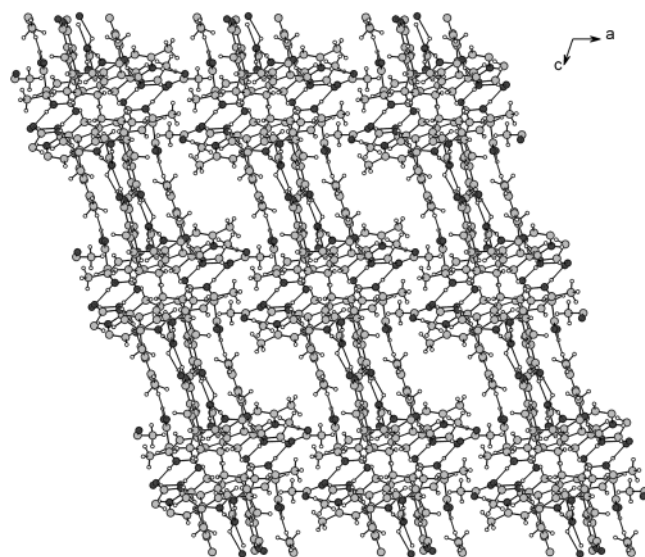


**FIGURE 11.** Crystal structure of  $(-)$ -**2**·**2AcOH**, aggregate **6**. View along the *b* axis showing four channels.

**5** and **6** were made with a Bruker Smart 1000 CCD diffractometer using synchrotron radiation at MAXLAB II,<sup>29</sup> Lund, Sweden ( $\lambda = 0.8860 \text{ \AA}$  for **5** and  $\lambda = 0.8797 \text{ \AA}$  for **6**). CCD data were extracted with the SAINT+ package, and intensity data were prepared with XPREP.<sup>30</sup>

(29) Cerenius, Y.; Ståhl, K.; Svensson, L. A.; Ursby, T.; Oskarsson, Å.; Albertsson, J.; Liljas, A. *J. Synchrotron Rad.* **2000**, *7*, 203–208.

(30) SAINT+, XPREP, Siemens Industrial Automation, Inc.: Madison, WI, 1995.

The structures were solved by direct methods and subsequent full-matrix least-squares refinement, including anisotropic thermal parameters for all non-hydrogen atoms. Hydrogen atoms were placed in calculated positions and not refined. Structure solution and refinement were carried out with the SIR-97<sup>31</sup> and SHELXL-97<sup>32</sup> program packages and refined against  $|F_2|$ . All data were collected at 210 K.

The absolute configuration of **6** was assigned based on the known configuration of  $(+)$ -**1**.

**Materials.**  $(\pm)$ - and  $(+)$ -(1*S*,5*S*)-Bicyclo[3.3.1]nonane-2,6-dione **1** were prepared according to the procedures described in the literature.<sup>21,33</sup> Hydrazine **3** was obtained in two steps from commercially available 4-hydroxy-6-methyl-2*H*-pyran-2-one according to the procedures described in the literature.<sup>16,17</sup>

**General Procedure for Synthesis of Bishydrazones.** Hydrazine **3** (ca. 2.1 equiv) was dissolved in boiling ethanol. To the resulting clear solution was added dione **1** (1 equiv), and the reaction mixture was heated under reflux for 4 h. The reaction mixture was cooled, and the resulting precipitate was filtered, washed with cold ethanol, and dried in vacuo to afford the corresponding hydrazones as a mixture of *E,E* and *E,Z* isomers, which were used without further purification.

**Bicyclo[3.3.1]nonane-2,6-dione Bis[(6-methyl-2-oxo-1,2-dihydro-4-pyridinyl) hydrazone] 4.** Obtained from 4-hydrazino-6-methyl-2(1*H*)-pyridinone **3** (190 mg, 1.38 mmol) and dione **1** (100 mg, 0.66 mmol) in ethanol (5 mL) as an off-white solid (230 mg, 88%): mp >320 °C; IR 3255, 3106, 2931,

(31) Altomare, A.; Burla, M. C.; Camalli, M.; Casciarano, G. L.; Giacovazzo, C.; Guagliardi, A.; Moliterni, A. G. G.; Polidori, G.; Spagna, R. *J. Appl. Crystallogr.* **1999**, *32*, 115–119.

(32) SHELXL97, Sheldrick, G. M. Göttingen, 1998.

(33) (a) Meerwein, H.; Schurmann, W. *Liebigs Ann. Chem.* **1913**, *397*, 196–250. (b) Lightner, D. A.; Chang, T. C.; Hefelfinger, D. T.; Jackman, D. E.; Wijekoon, W. M. D.; Givens, J. W., III. *J. Am. Chem. Soc.* **1985**, *107*, 7499–7508. (c) Quast, H.; Witzel, M. *Liebigs Ann. Chem.* **1993**, 699–700.

1624, 1227, 823  $\text{cm}^{-1}$ ;  $^1\text{H}$  NMR  $\delta$  10.62 (s, 2H), 9.35 (s, 0.27 H) and 9.19 (s, 1.73 H), 5.89 (s, 2H), 5.58 (s, 2H), 2.93–2.87 (dd,  $J = 6.5$  and  $17.3$  Hz, 2H), 2.72 (bs, 2H), 2.44–1.75 (m, 8H), 2.06 (s, 6H);  $^{13}\text{C}$  NMR (*E,E* isomer) 164.3, 155.1, 154.1, 144.8, 94.8, 90.5, 37.5, 33.2, 29.9, 23.7, 18.9;  $^{13}\text{C}$  NMR (*E,Z* isomer, only nonoverlapping signals are listed)  $\delta$  154.1, 144.7, 90.3, 37.1, 32.3, 31.3, 31.1, 28.7, 26.1, 23.5; MS  $m/z$  (%) 396 ( $[\text{M} + 2]^+$ , 28), 395 ( $[\text{M} + 1]^+$ , 100), 394 ( $[\text{M}]^+$ , 22), 307 (25), 298 (11), 154 (88), 136 (61), 107 (16), 89 (13); HRMS (FAB+) calcd for  $\text{C}_{21}\text{H}_{27}\text{N}_6\text{O}_2$  ( $[\text{M} + \text{H}]^+$ ) 395.2195, found 395.2196. Anal. Calcd for  $\text{C}_{21}\text{H}_{26}\text{N}_6\text{O}_2$ : C, 63.94; H, 6.64; N, 21.30. Found: C, 64.32; H, 6.81; N, 21.05.

(+)-(1*S*,5*S*)-**4**. Obtained from **3** (290 mg, 2.1 mmol) and (+)-(1*S*,5*S*)-dione **1** (150 mg, 0.99 mmol) in ethanol (8 mL) as off-white solid (320 mg, 82%): mp  $>320$  °C;  $[\alpha]_{\text{D}}^{20} = 123$  ( $c$  0.0068, 1-butanol).

**General Procedure for Synthesis of Methanocyclooctadiindoles.** A suspension of the appropriate bishydrazone in diphenyl ether was refluxed under nitrogen for 4 h. The cooled reaction mixture was diluted twice with diethyl ether, and the resulting precipitate was filtered, thoroughly washed with diethyl ether and hexane, and dried to afford the corresponding methanocyclooctadiindoles.

( $\pm$ )-**2,9-Diaza-3,10-dimethyl-1,8-dioxo-2,5,6,7,9,12,13,14-octahydro-6,13-methanocycloocta[1,2-*b*:5,6-*b'*]diindole 2**. Obtained from bishydrazone **4** (150 mg, 0.38 mmol) in diphenyl ether (5 mL). Recrystallization from glacial acetic acid afforded 110 mg (68%) of **2**·AcOH as off-white solid: mp  $>320$  °C; IR 3387, 3265, 1640, 1617  $\text{cm}^{-1}$ ;  $^1\text{H}$  NMR  $\delta$  10.94 (s, 2H), 10.43 (s, 2H), 5.98 (s, 2H), 3.22 (m, 2H), 2.92 (bs, 4H), 2.09 (s, 6H), 1.93 (s, 2H), 1.91 (s, 3H, AcOH);  $^{13}\text{C}$  NMR  $\delta$  172.3 (AcOH), 160.4, 138.9, 135.9, 133.1, 111.1, 111, 93.6, 29.9, 29.7, 27.3, 21.3 (AcOH), 18.8; MS  $m/z$  (%) 362 ( $[\text{M} + 2]^+$ , 21), 361 ( $[\text{M} + 1]^+$ , 82), 360 ( $[\text{M}]^+$ , 100), 359 ( $[\text{M} - 1]^+$ , 41), 307 (8), 199 (8), 154 (38), 136 (24); HRMS (FAB+) calcd for  $\text{C}_{21}\text{H}_{20}\text{N}_4\text{O}_2$  ( $[\text{M}]^+$ ) 360.1586, found 360.1586.

Crystals suitable for X-ray diffraction were obtained by recrystallization from DMF. Anal. Calcd for  $\text{C}_{21}\text{H}_{20}\text{N}_4\text{O}_2$ : C, 69.98; H, 5.59; N, 15.55. Found: C, 69.75; H, 5.74; N, 15.65.

**Crystallographic Data for ( $\pm$ )-**(2)**<sub>2</sub>·5DMF; Aggregate **5**.**  $\text{C}_{28.5}\text{H}_{37.5}\text{N}_{6.5}\text{O}_{4.5}$ , MW = 543.14, triclinic, space group *P1*,  $a =$

9.5265(2) Å,  $b = 11.831(3)$  Å,  $c = 13.775(3)$  Å,  $\alpha = 80.63(2)^\circ$ ,  $\beta = 73.94(2)^\circ$ ,  $\gamma = 80.70(2)^\circ$ ,  $V = 1460.9(5)$  Å<sup>3</sup>,  $Z = 2$ ,  $d_{\text{calc}} = 1.235$  g  $\text{cm}^{-3}$ ,  $F(000) = 760$ ,  $\lambda = 0.8860$  Å,  $\mu = 0.183$  mm<sup>-1</sup>,  $R_1 = 0.0802$ ,  $wR_2 = 0.2265$ , GOF = 1.036 for 3336 data ( $I > 2\sigma(I)$ ). Min/max residual electron density:  $-0.322/0.320$  e/Å<sup>3</sup>.

(-)-(**6R**,**13R**)-**2**. Obtained from bishydrazone (+)-**4** (300 mg, 0.76 mmol) in diphenyl ether (10 mL). Recrystallization from the glacial acetic acid afforded 250 mg (78%) of (-)-**2**·AcOH as beige solid: mp  $>320$  °C;  $[\alpha]_{\text{D}}^{20} = -612$  ( $c$  0.083, 2-propanol).

Crystals suitable for X-ray diffraction were obtained by vapor diffusion of ether to the solution of (-)-**2** in acetic acid.

**Crystallographic Data for (-)-**2**·2AcOH; Aggregate **6**.**  $\text{C}_{50}\text{H}_{56}\text{N}_8\text{O}_{12}$ , MW = 961.03, monoclinic, space group *P2*<sub>1</sub>,  $a = 12.507(3)$  Å,  $b = 16.748(3)$  Å,  $c = 13.978(3)$  Å,  $\beta = 108.98(3)^\circ$ ,  $V = 2768(3)$  Å<sup>3</sup>,  $Z = 2$ ,  $d_{\text{calc}} = 1.153$  g  $\text{cm}^{-3}$ ,  $F(000) = 1140$ ,  $\lambda = 0.8797$  Å,  $\mu = 0.179$  mm<sup>-1</sup>,  $R_1 = 0.088$ ,  $wR_2 = 0.222$ , GOF = 1.048 for 6468 data ( $I > 2\sigma(I)$ ). Min/max residual electron density:  $-0.385/1.456$  e/Å<sup>3</sup>.

**Acknowledgment.** This research was supported by the Swedish Institute (New Visby program), the Swedish Research Council, the MAXLAB in Lund, and partially by the Lithuanian Science and Studies Foundation. S.S. acknowledges The World Federation of Scientists for a Jerome and Isabella Karle scholarship. K.L. and L.Ö. would like to acknowledge the financial support from the Swedish Foundation for Strategic Research and the Gyllensvärd-Krappertup Foundation, and K.W. the Craafoord, the Lars-Johan Hierta, and the Magn. Bergvall Foundations, as well as the Royal Physiographic Society, Lund for generous support.

**Supporting Information Available:** General methods;  $^1\text{H}$  and  $^{13}\text{C}$  NMR spectra of **2** and **4**, and details of the X-ray analyses of aggregates **5** and **6** in CIF format. This material is available free of charge via the Internet at <http://pubs.acs.org>.

JO035869P